Biosensors and Bioelectronics 124–125 (2019) 53–58

Contents lists available at ScienceDirect

Biosensors and Bioelectronics

journal homepage: www.elsevier.com/locate/bios

A label-free electrochemical biosensor for ultra-sensitively detecting telomerase activity based on the enhanced catalytic currents of acetaminophen catalyzed by Au nanorods

Lei Wang, Tianjiao Meng, Guangshun Yu, Shasha Wu, Jingjing Sun, Huixian Jia, Huan Wang*, Xinjian Yang*, Yufan Zhang*

Key Laboratory of Analytical Science and Technology of Hebei Province, College of Chemistry and Environmental Science, Key Laboratory of Medicinal Chemistry and Molecular Diagnosis, Ministry of Education, Hebei University, 071002 Baoding, PR China

ARTICLE INFO

Keywords:
Telomerase activity
Electrochemical biosensor
Au nanorods
Ultra-sensitivity detecting

ABSTRACT

An electrochemical biosensor was designed for the determination of telomerase activity using an enzyme-free, PCR-free, and convenient electrochemical strategy. In this work, the electrochemical biosensor was constructed through the functionalization of Au nanorods with a carboxylic group (AuNRs-3) and subsequent immobilization with capture DNA (cDNA) for sensing telomerase activity. Upon telomerase triggered extension, the telomerase activity is related to the amount of the adsorbed electrocatalyst, leading to the different electrochemical signals for readout. Integrating with the efficient electrocatalysis of AuNRs-3-cDNA towards oxidation of acetaminophen, the prepared biosensor exhibits a wide dynamic correlation of telomerase activity from 1×10^2 to 1.04×10^7 HeLa cells mL^{-1} with a sensitivity of 2.68 HeLa cell mL^{-1} and the limit of detection was calculated to be 52.81 HeLa cells mL^{-1} under the optimal experimental conditions. Furthermore, the application of this electrochemical biosensor would provide the great potential for analysis of telomerase activity, revealing a powerful platform for early diagnosis of cancers.

1. Introduction

Telomerase is an enzyme that appends a repeating short sequence to the ends of chromosomes to protect the genetic material (Collins, 1996; Harley, 2008). It has been considered as a potentially sensitive biomarker for early cancer diagnosis (Collins and Mitchell, 2002; Shay and Wright, 2006). It is reported that the telomerase is over-expressed in more than 85% of malignant tumor cells, and thus highly sensitive detection of telomerase activity is crucially significant (Masutomi et al., 2003). Various strategies have been developed for telomerase activity analysis since the discovery of telomerase in 1985 by Greider and Blackburn (1985). The telomere repeat amplification protocol (TRAP) has been used as a conventional assay for detecting telomerase activity (Kim et al., 1994; Wu and Qu, 2015; Xiao and Yu, 2010; Xiao et al., 2010). However, it suffers from some drawbacks such as time-consuming, the risk of carry over contamination, and false positive readout. A variety of modified TRAP methods have been developed to overcome the shortcomings, but the practical usefulness is still limited. So far, many traditional methods have been reported for the detection of telomerase activity, including fluorescence (Ding et al., 2016; Zhang et al., 2016b), surface enhanced Raman scattering (Xu et al., 2016; Zong et al., 2014), and colorimetry (Wang et al., 2014; Zhang et al., 2016a). Although these methods can provide a useful platform for the detection of telomerase activity, the shortcomings such as high-cost, complex sample preparations and low-sensitivity have limited their applications. Therefore, the development of simple, highly sensitive and low cost approaches will potentially facilitate telomerase activity detection.

Electrochemical methods have attracted much attention recently for its promising applications in various biological sensing, due to merits of simple operation, low cost, high sensitivity and selectivity. For instance, Yi et al. reported an electrochemical telomerase biosensor with structure switching DNA probe for the detection of telomerase activity (Yi et al., 2014). Li et al. described the electrochemical telomerase biosensor based on a spired DNA tetrahedron (Li et al., 2015). However, the involvement of various DNA labeling makes these methods sophisticated. Thus, the development of a PCR-free and enzyme-free electrochemical method for efficient detection of telomerase activity would be very significant. An electrochemical telomerase biosensor on the basis of spherical nucleic acid gold triggered mimicry hybridization chain reaction was reported by Zhu and co-workers (Wang et al., 2015).

* Corresponding author.
E-mail addresses: huanwang@hbu.edu.cn (H. Wang), xjyang321@hbu.edu.cn (X. Yang), zyf@hbu.edu.cn (Y. Zhang).

https://doi.org/10.1016/j.bios.2018.09.098
Received 16 July 2018; Received in revised form 16 September 2018; Accepted 29 September 2018
Available online 09 October 2018
0956-5663/

Liu et al. described a sensitive electrochemical biosensor without modification or immobilization for label-free detection of telomerase activity (Liu et al., 2017). Ju's group designed an electrochemical biosensor combined platinum nanoparticle with metal-organic frameworks for the detection of telomerase activity (Ling et al., 2016).

Au nanorods (AuNRs) are one kind of elongated and anisotropic gold nanoparticles, which has drawn widespread concern for its excellent conductivity, high surface area-to-volume, good catalytic activity and strong adsorption capacity. AuNRs are sensitive to the surrounding dielectric constant and enhance the signal amplification of biosensing (Akhtar et al., 2018; Xiao and Yu, 2010; Xiao et al., 2010; Zhu et al., 2013). Ordered mesoporous carbon (OMC) materials are essential for numerous modern applications because of their favourable properties, including unique mesoporous structure, exceptional chemical inertness, large specific surface area, and good electrical conductivity (Kong et al., 2017; Wang et al., 2018; Zhang et al., 2014c; Zhang et al., 2015).

Inspired by the aforementioned works, we reported an enzyme-free and PCR-free electrochemical approach. In this method, AuNRs were functionalized with a carboxylic group (AuNRs-3), and sequentially immobilized with capture DNA (cDNA) as a signal probe for sensing telomerase activity. As shown in Scheme 1, telomerase primer (TS) was attached onto the glassy carbon electrode (GCE) surface, which can be extended $(TTAGGG)_n$ in the presence of the dNTPs and telomerase extracts and then hybridized with the AuNRs-3-cDNA probe. Upon telomerase triggered extension, the telomerase activity is related to the amount of the adsorbed electrocatalyst, leading to the different electrochemical signals for readout towards acetaminophen (AP). The designed approach can measure the telomerase activity with wide dynamic range, high sensitivity, and low limit of detection. This facile and reliable strategy was offered for detecting telomerase activity.

2. Experimental

2.1. Reagents and materials

(3-Aminopropyl) trimethoxysilane (APTES), hexadecyl trimethyl ammonium bromide (CTAB), ascorbic acid, silver nitrate ($AgNO_3$), tetraethyl orthosilicate (TEOS), triethylamine, dimethyl sulfoxide (DMSO), 2-mercaptoethano, succinic anhydride, 3-[(3-cholamidopropyl) dimethylammonio] − 1-propanseulfonic acid (CHAPS), phenylmethylsulfonyl fluorid (PMSF), ethylene glycol bis (2-aminoethyl ether)-*N,N,N,N*-tetraacetic acid (EGTA), Tris-(hydroxymethyl) aminomethane (Tris), Tween 20, glycerol, magnesium chloride ($MgCl_2$), sucrose, bovine serum albumin (BSA), and tetrachloroauric acid ($HAuCl_4$) were all purchased from Shanghai Macklin Biochemical Co. Ltd. The deoxynucleotide mixture (dNTPs), hydrochloride (EDAC), *N*-hydroxysuccinimide (NHS), and all DNA oligonucleotides were obtained by Sangon Biotechnology Ins. (Shanghai, China). 6-Mercapto-1-hexanol (MCH) was offered by Aladdin Inc. (Shanghai, China). Ethanol absolute, sodium borohydride for synthesis ($NaBH_4$), nitric acid, potassium chloride (KCl), methanol, hydrofluoric acid (HF), sodium hydroxide (NaOH) and nitric acid (HNO_3) were received from Beijing Chemical Co. Ltd. Pluronic P123 (nonionic triblock copolymer $EO_{20}PO_{70}EO_{20}$) was obtained from Sigma-Aldrich. Other reagents employed were all of analytical reagent grade. All solutions were prepared with nanopure water (> 18 MΩ, Millipore). The sequences are as follows:

TS: 5′-NH_2C_6-TTTTTTTTTTAATCCGTCGAGCAGAGTT-3′

Capture DNA (cDNA): 5′-NH_2C_6-TTTTTTTTTTAACCCTAACCCT-3′

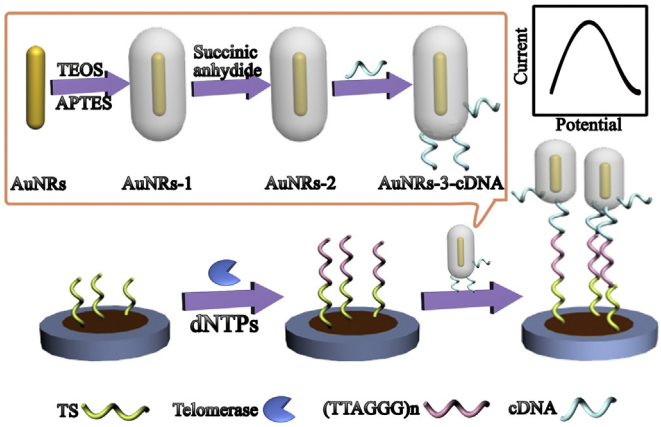

Scheme 1. Schematic of sensing principle for the electrochemical detection of telomerase activity.

2.2. Apparatus and characterization

Morphological properties of the materials were recorded using scanning electron microscopy (SEM, PhilipsXL-30 ESEM) and transmission electron microscopy (TEM, JEM-2100F). Flourier-transform infrared (FT-IR) spectra were characterized on Nicolet Magna 560 FT-IR spectrometer. Electrochemical measurements were performed with AUTOLAB Electrochemical Workstation (Metrohm Instruments, Switzerland) in three-electrode system, including a glassy carbon electrode (GCE) as working electrode, a platinum wire auxiliary electrode, and an Ag/AgCl (insaturated KCl solution) reference electrode.

2.3. Preparation of carboxylic acid-functionalized Au nanorods

The carboxylic acid-functionalized Au nanorods (AuNRs-3) were prepared by the reported method with minor modifications (Yang et al., 2012). Briefly, the freshly prepared ice-cold $NaBH_4$ (0.01 M, 0.02 mL) was added to the mixed solution consisting of $HAuCl_4$ (0.50 mM, 0.20 mL), and CTAB (0.20 M, 0.20 mL) under vigorous agitation, which resulted in the formation of a brownish yellow seed solution. The growth solution was prepared by mixing together in 100 mL flask 20.00 mL of 0.20 M CTAB, 1.12 mL of 4.00 mM $AgNO_3$, 1.30 mL of 23 mM $HAuCl_4$, and 19.00 mL of Milli-Q water, followed by the addition of ascorbic acid (0.40 mL, 0.08 M). Afterwards, 0.36 mL seed solution was added. The color of the solution gradually changed within 15–25 min. The temperature of the growth medium was kept constant at 27–30 °C during the full procedure. Then, the as-prepared samples were centrifuged at 12,500 rpm for 25 min and the precipitate was redispersed by 10.00 mL of Milli-Q water. To get mesoporous silica-encapsulated AuNRs (AuNRs-1), 0.10 mL of 0.1 M NaOH solution and 0.09 mL of TEOS (20%) were added under stirring. In order to get amido modified AuNRs (AuNRs-2), 2 μL of APTES in 20 μL methanol was added under stirring. Red precipitate was got after centrifugation twice, and then refluxed for 1 h in a solution of 0.10 mL of HCl (37%) and 10 mL of methanol followed by extensively washing with hot methanol. The carboxylic acid-functionalized particles (henceforth AuNRs-3 for convenience) were prepared by reacting succinic anhydride (0.04 g) with AuNRs-2 (2.00 mg) in DMSO solution in the presence of triethylamine (0.10 g). The final sample was collected by centrifugation, washed with ethanol, and dried in a vacuum at 60 °C.

2.4. Bioconjugation of AuNRs-3 with cDNA

AuNRs-3-cDNA was prepared via the conjugation between -COOH groups of AuNRs-3 and $-NH_2$ groups of cDNA. AuNRs-3 (1.60 mg) was added to EDC and NHS (10 mg/mL, 0.80 mL) in ultrapure water and reacted for 20 min at room temperature. Then, the aqueous solution of DNA (10 μM, 0.50 mL) was injected into the above aqueous solution, reacted for 6 h at room temperature, and centrifuged at 12,500 rpm for 25 min. The resulting AuNRs-3-cDNA conjugate was resuspended in PBS (0.1 M, pH 7.4) and stored at 4 °C prior to use.

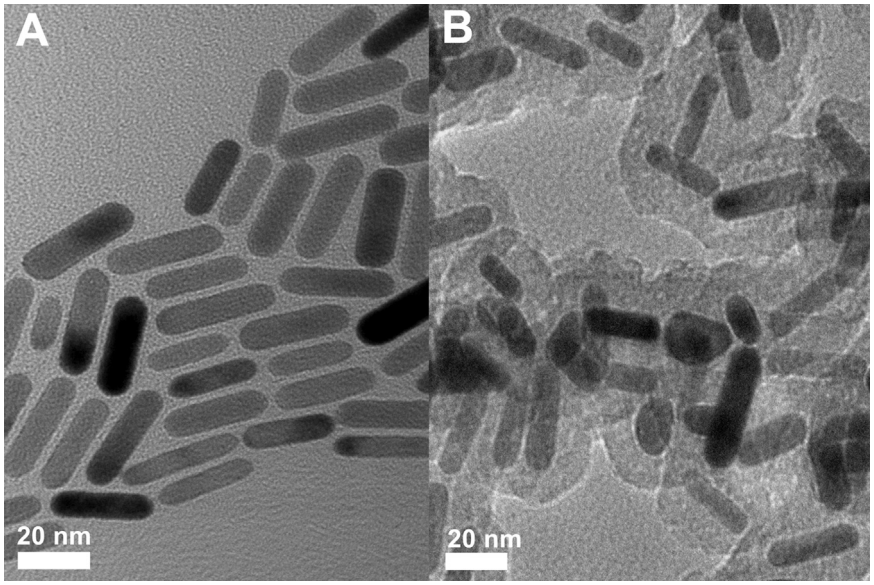

Fig. 1. TEM images of the as-synthesized AuNRs (A) and AuNRs-*1* (B).

2.5. Preparation of acid-functionalized OMC

OMC was synthesized using SBA-15 mesoporous silica as template by a nanohard-templating approach according to the method reported by Ryoo et al. (1999). The acid-functionalized OMC samples were prepared by dispersing 0.30 g OMC powder in the 50.00 mL solution of 1 M HNO_3 and being heated at 90 °C for 6 h under refluxing conditions. The sample was washed with water until the pH of the filtrate water became neutral, and centrifuged at 9500 rpm for 6 min. Acid-functionalized OMC sample was obtained was dried in air at 100 °C.

2.6. Agarose gel electrophoresis

The agarose gels were prepared with 1% agarose in Tris-Acetate EDTA buffer (TAE buffer). All of the samples (10 μM TS solution/cDNA/the mixtures of 10 μM TS solution and cell extract/the mixtures of 10 μM TS solution and heated extract/the mixtures of 10 μM TS solution and cDNA/the mixtures of 10 μM TS solution, cell extract and cDNA) were suspended in buffer (5 μL sample solution + 1 μL loading buffer) and added to agarose gel subsequently. The gel electrophoresis was run for 35 min at 85 mV and then for gel imaging. The feasibility of the method was verified by agarose gel electrophoresis (Fig. S1).

2.7. Cell culture and extraction of telomerase

HeLa (Human cervix adenocarcinoma), MCF-7, A549, MDA-MB-231 cells were cultured using Dulbecco's Modified Eagle Medium (DMEM) supplemented with antibiotics (100 U mL^{-1}, streptomycin; 100 U mL^{-1}, penicillin) and 10% fetal bovine serum (FBS) at 37 °C with 5% CO_2.

Briefly, about 1.04×10^7 cells were dispersed in 14.0 mL EP tube, washed twice with ice-cold PBS (0.1 M, pH 7.4), and centrifuged at 2000 rpm for 5 min at 4 °C. And then, the cells were resuspended in 2.0 mL of ice-cold lysis buffer, including Tris-HCl (10 mM pH 7.5), $MgCl_2$ (1 mM), EGTA (1 mM), PMSF (0.1 mM), 2-mercaptoethano (5 mM), CHAPS (0.5%), and glycerol (10%). The mixture was kept on ice for 30 min, and centrifuged for 20 min at 12,000 rpm. The cleared lysate was carefully transferred into a fresh EP tube, immediately use for telomerase assay or frozen at −80 °C.

2.8. GCE treatment

Prior to the modification, the GCE (3 mm diameter) was polished sequentially with alumina slurry of 1, 0.3 and 0.05 μm, respectively, followed by successive sonication with nanopure water and ethanol. Subsequently, 2 mg of acid-functionalized OMC were dispersed into 1 mL of water to give homogeneous suspension upon bath sonication. Then, 5 μL of the suspension was dip-coated onto GCE surface. After dried, EDC and NHS (10 mg/mL, 20 μL) was cast onto the GCE surface for 30 min. Subsequently, the GCE was immersed in 0.5 μM of telomerase primer at 4 °C, and rinsed with 10 mM of Tris-HCl buffer (pH 8.3). The electrode was further incubated with 1 mM of MCH for 2 h, and rinsed thoroughly with 10 mM of Tris-HCl buffer (pH 8.3).

2.9. Construction of electrochemical biosensor and electrochemical detection

The pretreated GCE was immersed in 100 μL of extension solution containing 50 μL of telomerase extracts and 2 mM of dNTPs mixture in 1 × TRAP buffer, containing Tris-HCl (20 mM pH 8.3), $MgCl_2$ (1.5 mM), KCl (63 mM), Tween 20 (0.005%), EGTA (1 mM), and BSA (0.1 mg mL^{-1}), and incubated at 37 °C for 30 min to allow the extension reaction by telomerase. Subsequently, 10 μL of AuNRs-3-cDNA (2 mg/mL) were dip-coated onto the resulting electrode surface and incubated at 37 °C for 30 min. The modified electrode was then placed in a PBS solution (0.1 M, pH 7.4) for differential pulse voltammetry (DPV) measurement. The DPV was carried out from − 1.0 to 1.0 V with the parameters of step potential 5 mV, modulation amplitude 25 mV, modulation time 0.05 s and interval time 0.5 s.

3. Results and discussion

3.1. Characterization of the as-prepared samples

The morphologies of AuNRs and AuNRs-1 were characterized by TEM analysis. A typical TEM image of AuNRs is presented in Fig. 1A, which shows that the AuNRs are uniformly dispersed with the average length of 30 nm. To contain the AuNRs within the silica shells, the modified sol-gel method was used for the preparation of the mesoporous silica-encapsulated Au nanorods. The shape of the AuNRs-1 was shown in Fig. 1B, demonstrating that the AuNRs were successfully encapsulated in situ by silica shell.

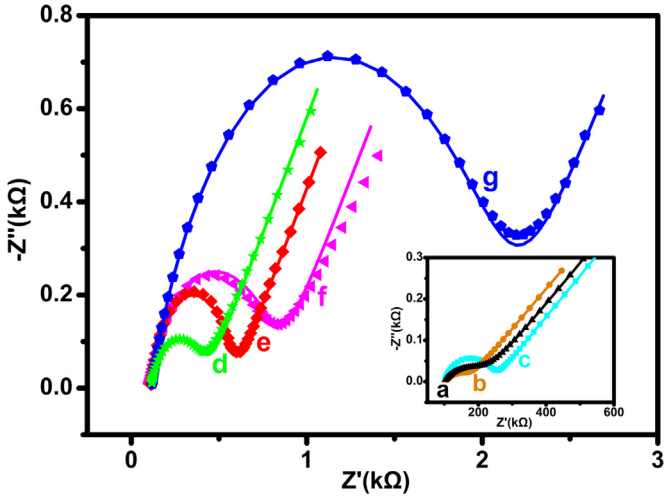

Fig. 2. EIS response of the different modification process of the electrode interface in the solution containing 5.0 mM of $K_3Fe(CN)_6/K_4Fe(CN)_6$ from 0.1 Hz to 100.0 kHz: bare GCE (a), AuNRs/GCE (b), acid-functionalized OMC/GCE (c), TS/GCE (d), (extract + TS)/GCE (e), AuNRs-3-cDNA/GCE (f), and (extract + TS/AuNRs-3-cDNA)/GCE (g), respectively.

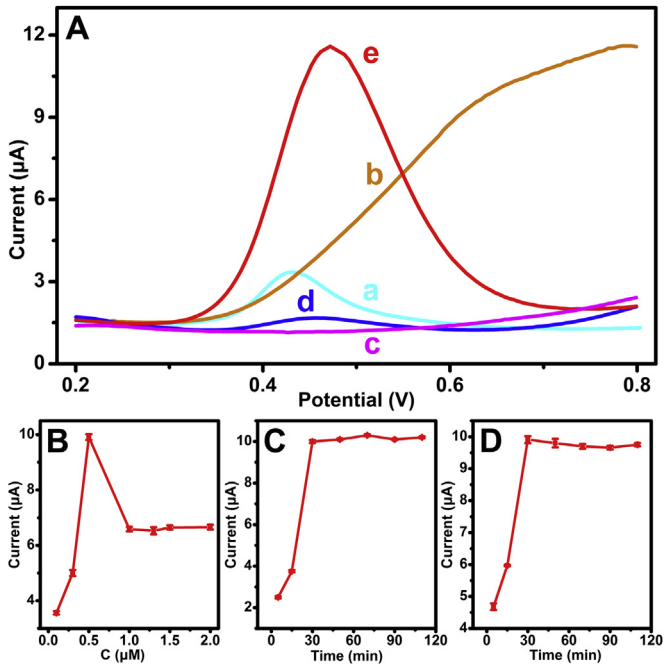

Fig. 3. DPV responses of bare GCE (a), TS/GCE (b), TS-extract/GCE (c), (heated extract + TS/AuNRs-3-cDNA)/GCE (d), and (extract + TS/AuNRs-3-cDNA)/GCE (e) in the presence of AP (2 μM) (A). The influence of concentration of TS primer (B), incubation time for telomerase extension reaction (C), and hybridization reaction time between AuNRs-3-cDNA and the extended TS (D) on the current response to telomerase activity of 1×10^5 cell mL^{-1}.

The surface functionalization of various AuNRs was studied by FT-IR spectroscopy (Fig. S2). Both AuNRs and AuNRs-*x* present the absorption band at around 1485 and 1635 cm^{-1}, which is corresponding to the acylamide vibration within the attached succinic acid molecules. The emerging absorption band at around 1705 cm^{-1} in the sample can be attributed to C=O stretching of the carboxyl groups.

3.2. Electrochemical behavior of different electrode materials

Electrochemical impedance spectra (EIS) measurements were carried out to investigate the changes on the electrode surface employing $Fe[(CN)_6]^{4-/3-}$ couple as the redox probe in the supporting electrolyte solution. Since the negative charges of DNA prevent repelling electrons from approaching the electrode surface, it is expected that the diameter of the Nyquist plot should increase along with the equivalent amount of DNA. As a whole, the charge transfer resistance (R_{ct}) values also increased stepwise along with the extension process (Table S1). As shown in Fig. 2, the bare GCE (curve a), AuNRs/GCE (curve b), and acid-functionalized OMC/GCE (curve c) exhibit the very small semicircle part at high frequencies, which demonstrated good electrochemical activity and fast charge-transfer process. Subsequently, the GCE was immersed in TS and passivation of the surface with MCH shows an obviously increase of R_{ct} value (curve d). After telomerase extension, the R_{ct} value is 461.3 Ω (curve e). The R_{ct} value of AuNRs-3-cDNA /GCE is 716.9 Ω (curve f). Furthermore, the hybridization between AuNRs-3-cDNA and telomere repeats makes the value of R_{ct} increase to 1997.0 Ω (curve g). The measure of impedance from curves a to g becomes larger and larger due to the higher density of DNA. These results confirm the successful fabrication of the biosensor.

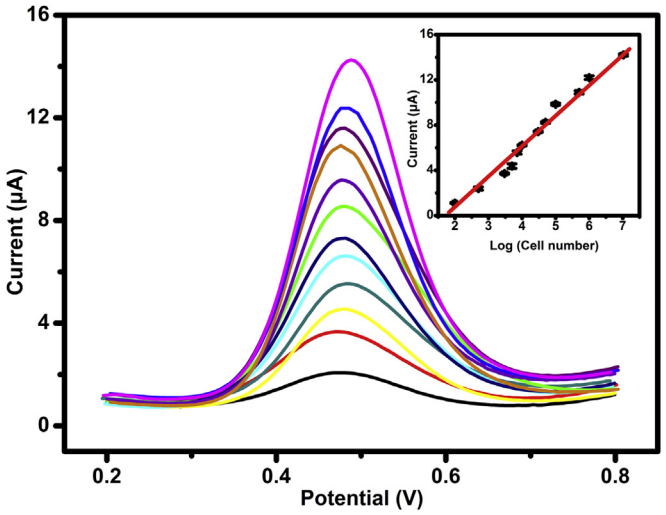

Fig. 4. DPV responses of a range of HeLa cell numbers (from top to down): 1.04×10^7, 1×10^6, 5×10^5, 1×10^5, 5×10^4, 3×10^4, 1×10^4, 7×10^3, 5×10^3, 3×10^3, 5×10^2, 1×10^2. Inset: the corresponding DPV signals vs. the logarithm of HeLa cell numbers.

The electrochemical behavior of different electrodes towards AP is investigated in Fig. 3A. A typical oxidation peak was observed at around 0.45 V on bare GCE (curve a). There is no peak current after the GCE was immersed in TS and passivation of the surface with MCH (curve b). When treatment with cell extract in the presence of dNTPs (curve c), no peak current was observed. After treatment with the heated-treated cell extract, the small peak current was obtained due to the nonspecific adsorption between the electrode surface and AuNRs-3-cDNA (curve d). However, the proposed biosensor exhibits obvious increased peak current because of hybridization between AuNRs-3-cDNA and telomere repeats (curve e). The results indicated the viability of the fabricated biosensor for the evaluation of telomerase activity.

3.3. Optimization of the detection conditions

To ensure high sensitivity and hybridization efficiency, some experiment parameters including the concentration of TS, incubation time, and hybridization time were optimized. In Fig. 3B, with the concentration of TS increased, the current reached a maximum at 0.5 μM of TS and then decreased, which indicated that TS on the electrode surface could hinder extension of telomerase. Thus, 0.5 μM of TS was selected as the optimal concentration of TS. The influence of incubation time for telomerase extension reaction was also

Table 1
Comparison of analytical performance for the detection of telomerase activity by as-proposed method and other reported in the literature.

Strategy	Detection mode	Linear range	Limit of detection	Ref.
Hemin-graphene conjugates-based biosensor	Colorimetry and UV-vis	1×10^2-2×10^4 HeLa cells mL^{-1}	60 HeLa cells	Xu et al. (2017)
Difunctional gold NPs	UV-vis	6×10^3-9.4×10^4 HeLa cells mL^{-1}	6000 HeLa cells mL^{-1}	Duan et al. (2014)
G-quardruplex/hemin controlled aggregation of Au NPs	UV-vis	2.7×10^4-1.9×10^5 HeLa cells mL^{-1}	2.7×10^4 HeLa cells mL^{-1}	Sharon et al. (2014)
Primer-modified Au NPs	UV-vis	0–8×10^3 HeLa cells mL^{-1}	1000 HeLa cells mL^{-1}	Wang et al. (2012)
8–17 DNAzyme and a hairpin shaped probe	Fluorescence	2×10^2-1×10^5 HeLa cells	200 HeLa cells	Tian et al. (2013)
Multifunctional Au NPs-based ECL sensor	ECL	3.13×10^2-1×10^4 cells	148 cells	Zhang et al. (2014a)
Bifunctionalized luminal-gold NPs	ECL	1×10^2-9×10^3 cells	62 cells	Zhang et al. (2014b)
Via enzymatic etching of gold nanorods assay	Colorimetry	2×10^2-1.5×10^4 HeLa cells mL^{-1}	90 HeLa cells	Yang et al. (2017)
Label-free electeochemical assay	EIS	1×10^3-1×10^5 HeLa cells mL^{-1}	1000 HeLa cells mL^{-1}	Yang et al. (2011)
Structure-switching DNA-based biosensor	DPV	1×10^2-6×10^4 HeLa cells mL^{-1}	100 HeLa cells mL^{-1}	Yi et al. (2014)
AuNRs-3 composite	DPV	1×10^2-1.04×10^7 HeLa cells mL^{-1}	52.81 HeLa cells mL^{-1}	This work

investigated. It can be seen from Fig. 3C, the current signal increased with the extension of incubation time for telomerase extension reaction and remained stable over 30 min. Therefore, 30 min were chosen as the optimal incubation time. Fig. 3D illustrated the effect of hybridization time between AuNRs-3-cDNA and telomere repeats on the response current. The current signal increased with the increase of hybridization time, and there was almost no change over 30 min. As a result, hybridization time of 30 min was selected as the optimal experimental time in this work.

3.4. Electrochemical detection of telomerase activity

The electrochemical signals in response to different concentrations of HeLa cells were evaluated with DPV measurements under the optimal experimental conditions. With the increase of concentrations of HeLa cells, more AuNRs-3-cDNA was obtained on the electrode surface, resulting in higher electrochemical signals. The calibration curve shown in Fig. 4 reveals that the changes of DPV peak currents were proportional to the logarithm of the HeLa cell concentration, with a good liner relationship from 1×10^2 to 1.04×10^7 HeLa cell mL^{-1}. The limit of detection was calculated to be 52.81 HeLa cell mL^{-1}, which was comparable with the biosensors reported by other groups (Table 1).

3.5. Repeatability, stability, and real sample analysis

The repeatability was investigated in three repetitive assays of 3×10^3, 1×10^4, and 1×10^5 HeLa cells. The relative standard deviation (RSD) of 4.98%, 5.18%, 8.87% were obtained, which suggested the sensor has excellent repeatability. Furthermore, the biosensor remained at 95.23% of the original value after it was stored in the fridge at 4 °C for 30 days, revealing good satisfactory stability of the developed sensor.

To further evaluate the practical applicability of the proposed biosensor, human serum sample assay was estimated. The detection results are shown in Table S2. The recoveries were 94.3–100.0%, indicating that the proposed biosensor is able to detect telomerase activity in real samples.

4. Conclusions

In summary, we successfully developed an electrochemical biosensor based on the AuNRs incorporated within a silica framework that was surface-functionalized with capture cDNA for sensitive electrochemical detection of telomerase activity. TS was attached onto the OMC modified GCE due to the conjugation between -NH_2 groups of TS primer and -COOH groups of OMC, which can be extended $(TTAGGG)_n$ in the presence of the dNTPs and telomerase extracts and then hybridized with the AuNRs-3-cDNA. The hybridization between AuNRs-3-cDNA electrocatalyst and the extended part on the sensor surface could lead to the significantly amplified electrocatalytic current towards AP. Upon telomerase triggered extension, the telomerase activity is related to the amount of the adsorbed electrocatalyst, leading to the different electrochemical signals for readout. The proposed method was enzyme-free and PCR-free without the requirement of any additional separation steps. Considering the outstanding sensitivity, wide dynamic range, and low limit of detection, the use of this construction strategy of electrochemical biosensor for the detection of telomerase activity is very ingenious. Meanwhile, the construction of electrochemical biosensor has the potential applications for bioassays and paves a new way for the detection of various biomolecules.

Acknowledgements

The authors gratefully acknowledge the support from the National Natural Science Foundation of China (No. 21505031 and No. 21603051) and the Natural Science Foundation of Hebei Province (No. B2016201018 and No. B2018201214).

Appendix A. Supporting information

Supplementary data associated with this article can be found in the online version at doi:10.1016/j.bios.2018.09.098.

References

Akhtar, M.H., Hussain, K.K., Gurudatt, N.G., Chandra, P., Shim, Y.B., 2018. Biosens. Bioelectron. 116, 108–115.
Collins, K., 1996. Curr. Opin. Cell Biol. 8, 374–380.
Collins, K., Mitchell, J.R., 2002. Oncogene 21, 564–579.
Ding, C., Li, X., Wang, W., Chen, Y., 2016. Biosens. Bioelectron. 83, 102–105.
Duan, R., Wang, B., Zhang, T., Zhang, Z., Xu, S., Chen, Z., Lou, X., Xia, F., 2014. Anal. Chem. 86, 9781–9785.
Greider, C.W., Blackburn, E.H., 1985. Cell 43, 405–413.
Harley, C.B., 2008. Nat. Rev. Cancer 8, 167–179.
Kim, N., Piatyszek, M., Prowse, K., Harley, C., West, M., Ho, P., Coviello, G., Wright, W., Weinrich, S., Shay, J., 1994. Science 266, 2011–2015.
Kong, X.Y., Wang, Y.Y., Zhang, Q.Q., Zhang, T.R., Teng, Q.Q., Wang, L., Wang, H., Zhang, Y.F., 2017. J. Colloid Interface Sci. 505, 615–621.
Li, Y., Wen, Y., Wang, L., Liang, W., Xu, L., Ren, S., Zou, Z., Zuo, X., Fan, C., Huang, Q., Liu, G., Jia, N., 2015. Biosens. Bioelectron. 67, 364–369.
Ling, P., Lei, J., Jia, L., Ju, H., 2016. Chem. Commun. 52, 1226–1229.
Liu, X., Wei, M., Xu, E., Yang, H., Wei, W., Zhang, Y., Liu, S., 2017. Biosens. Bioelectron. 91, 347–353.
Masutomi, K., Yu, E.Y., Khurts, S., Ben-Porath, I., Currier, J.L., Metz, G.B., Brooks, M.W., Kaneko, S., Murakami, S., DeCaprio, J.A., Weinberg, R.A., Stewart, S.A., Hahn, W.C., 2003. Cell 114, 241–253.
Ryoo, R., Joo, S.H., Jun, S., 1999. J. Phys. Chem. B 103, 7743–7746.
Sharon, E., Golub, E., Niazov-Elkan, A., Balogh, D., Willner, I., 2014. Anal. Chem. 86, 3153–3158.
Shay, J.W., Wright, W.E., 2006. Nat. Rev. Drug Discov. 5, 577–584.
Tian, T., Peng, S., Xiao, H., Zhang, X., Guo, S., Wang, S., Zhou, X., Liu, S., Zhou, X., 2013. Chem. Commun. 49, 2652–2654.
Wang, J.S., Wu, L., Ren, J.S., Qu, X.G., 2012. Small 8, 259–264.
Wang, J.S., Wu, L., Ren, J.S., Qu, X.G., 2014. Nanoscale 6, 1661–1666.
Wang, L., Teng, Q.Q., Sun, X.T., Chen, Y.T., Wang, Y.M., Wang, H., Zhang, Y.F., 2018. J. Colloid Interface Sci. 512, 127–133.
Wang, W.J., Li, J.J., Rui, K., Gai, P.P., Zhang, J.R., Zhu, J.J., 2015. Anal. Chem. 87, 3019–3026.
Wu, L., Qu, X.G., 2015. Chem. Soc. Rev. 44, 2963–2997.
Xiao, N., Yu, C., 2010a. Anal. Chem. 82, 3659–3663.

Xiao, Y., Dane, K.Y., Uzawa, T., Csordas, A., Qian, J., Soh, H.T., Daugherty, P.S., Lagally, E.T., Heeger, A.J., Plaxco, K.W., 2010b. J. Am. Chem. Soc. 132, 15299–15307.
Xu, L., Zhao, S., Ma, W., Wu, X., Li, S., Kuang, H., Wang, L., Xu, C., 2016. Adv. Funct. Mater. 26, 1602–1608.
Xu, X., Wei, M., Liu, Y., Liu, X., Wei, W., Zhang, Y., Liu, S., 2017. Biosens. Bioelectron. 87, 600–606.
Yang, H., Liu, A., Wei, M., Liu, Y., Lv, B., Wei, W., Zhang, Y., Liu, S., 2017. Anal. Chem. 89, 12094–12100.
Yang, W., Zhu, X., Liu, Q., Lin, Z., Qiu, B., Chen, G., 2011. Chem. Commun. 47, 3129–3131.
Yang, X.J., Liu, X., Liu, Z., Pu, F., Ren, J.S., Qu, X.G., 2012. Adv. Mater. 24, 2890–2895.
Yi, Z., Wang, H., Chen, K., Gao, Q., Tang, H., Yu, R., Chu, X., 2014. Biosens. Bioelectron. 53, 310–315.
Zhang, H.R., Wang, Y.Z., Wu, M.S., Feng, Q.M., Shi, H.W., Chen, H.Y., Xu, J.J., 2014a. Chem. Commun. 50, 12575–12577.
Zhang, H.R., Wu, M.S., Xu, J.J., Chen, H.Y., 2014b. Anal. Chem. 86, 3834–3840.
Zhang, L., Zhang, S., Pan, W., Liang, Q., Song, X., 2016c. Biosens. Bioelectron. 77, 144–148.
Zhang, X., Cheng, R., Shi, Z., Jin, Y., 2016b. Biosens. Bioelectron. 75, 101–107.
Zhang, Y.F., Bo, X.J., Nsabimana, A., Luhana, C., Wang, G., Wang, H., Li, M., Guo, L.P., 2014c. Biosens. Bioelectron. 53, 250–256.
Zhang, Y.F., Bo, X.J., Nsabimana, A., Munyentwali, A., Han, C., Li, M., Guo, L.P., 2015. Biosens. Bioelectron. 66, 191–197.
Zhu, Y., Chandra, P., Shim, Y.B., 2013. Anal. Chem. 85, 1058–1064.
Zong, S., Wang, Z., Chen, H., Hu, G., Liu, M., Chen, P., Cui, Y., 2014. Nanoscale 6, 1808–1816.